

Experimental study of the astrophysically important $^{23}\text{Na}(\alpha, p)^{26}\text{Mg}$ and $^{23}\text{Na}(\alpha, n)^{26}\text{Al}$ reactions

M. L. Avila,^{1,*} K. E. Rehm,¹ S. Almaraz-Calderon,² A. D. Ayangeakaa,¹ C. Dickerson,¹ C. R. Hoffman,¹ C. L. Jiang,¹ B. P. Kay,¹ J. Lai,³ O. Nusair,¹ R. C. Pardo,¹ D. Santiago-Gonzalez,^{1,3} R. Talwar,¹ and C. Ugalde¹

¹Physics Division, Argonne National Laboratory, Argonne, Illinois 60439, USA

²Department of Physics, Florida State University, Tallahassee, Florida 32306, USA

³Department of Physics and Astronomy, Louisiana State University, Baton Rouge, Louisiana 70803, USA

(Received 12 August 2016; revised manuscript received 27 October 2016; published 19 December 2016)

The $^{23}\text{Na}(\alpha, p)^{26}\text{Mg}$ and $^{23}\text{Na}(\alpha, n)^{26}\text{Al}$ reactions are important for our understanding of the ^{26}Al abundance in massive stars. The aim of this work is to report on a direct and simultaneous measurement of these astrophysically important reactions using an active target system. The reactions were investigated in inverse kinematics using ^4He as the active target gas in the detector. We measured the excitation functions in the energy range of about 2 to 6 MeV in the center of mass. We have found that the cross sections of the $^{23}\text{Na}(\alpha, p)^{26}\text{Mg}$ and the $^{23}\text{Na}(\alpha, n)^{26}\text{Al}$ reactions are in good agreement with previous experiments and with statistical-model calculations. The astrophysical reaction rate of the $^{23}\text{Na}(\alpha, n)^{26}\text{Al}$ reaction has been reevaluated and it was found to be larger than the recommended rate.

DOI: [10.1103/PhysRevC.94.065804](https://doi.org/10.1103/PhysRevC.94.065804)

I. INTRODUCTION

The importance of the radioisotope ^{26}Al in the fields of γ -ray astronomy and chemical cosmology has been well established over the past few years. The γ rays from the decay of ^{26}Al are direct evidence of the continuing nucleosynthesis in stars, providing a unique way of testing the predictive power of theoretical stellar models. Since the half-life of ^{26}Al (7.2×10^5 years) is small compared to the time scales of galactic chemical evolution ($\approx 10^{10}$ years), the ^{26}Al found in the interstellar medium is the outcome of relatively recent nucleosynthesis in the galaxy. ^{26}Al can be traced by measuring the 1.809 MeV γ -ray line associated with its radioactive decay. A complete sky map of the corresponding γ -ray emission has been produced using data gathered by instruments on board the COMPTEL [1] and INTEGRAL [2] satellites. Although the precise source of ^{26}Al is not completely understood, the observations by COMPTEL and INTEGRAL showed that the ^{26}Al distribution is confined towards the galactic disk, which strongly suggest massive stars ($M > 8M_\odot$) as one of the most likely production sites.

Sensitivity studies performed by Iliadis *et al.* [3] used around 900 nuclear reaction network calculations to determine the nuclear reactions that affect the ^{26}Al abundance in massive stars. In their work, three different massive star sites were investigated: explosive neon-carbon burning, convective shell carbon burning, and convective core hydrogen burning. The $^{23}\text{Na}(\alpha, p)^{26}\text{Mg}$ reaction and four other reactions were suggested as prime targets for experimental measurements. The $^{23}\text{Na}(\alpha, p)^{26}\text{Mg}$ reaction is an important proton source for producing ^{26}Al from ^{25}Mg . Improved experimentally determined reaction rates for the $^{23}\text{Na}(\alpha, p)^{26}\text{Mg}$ reaction were needed at about 2.3 GK for explosive Ne/C burning and 1.4 GK for convective shell C/Ne burning. Although the $^{23}\text{Na}(\alpha, p)^{26}\text{Mg}$ reaction was measured in Refs. [4,5], the

authors of Ref. [3] did not consider the data reliable, due to problems associated with degradation of the NaCl targets used in the experiments, and the reaction rates used in their calculations were instead based on theoretical estimates.

In Ref. [6], the $^{23}\text{Na}(\alpha, p)^{26}\text{Mg}$ reaction was measured in inverse kinematics using ^{23}Na beams of different energies on a cryogenic ^4He gas target. The energy range investigated in Ref. [6] ranged from 1.36 to 2.42 MeV in the center-of-mass system. This study reported a reaction rate which was higher than the recommended rate by about a factor of 40. This result would have significant implications for the ^{26}Al production, suggesting that the abundance of ^{26}Al was larger by a factor of about 3. More recently, this reaction was remeasured [7,8]. The experiment reported in Ref. [7] studied the excitation function in the center-of-mass energy range of 1.28 to 3.15 MeV using inverse kinematics with a ^{23}Na beam impinging on a ^4He gas target, similar to the experiment of Ref. [6]. The experiment of Ref. [8] was performed in normal kinematics with a ^4He beam of energies between 1.99 and 2.94 MeV (1.7–2.5 MeV in the center of mass) bombarding a carbon-backed NaCl target. The measurements of Refs. [7,8] were found to be in good agreement with each other and with statistical-model calculations; however, they were in disagreement with the large cross sections found in Ref. [6]. Due to these discrepancies, the data of Ref. [6] were reanalyzed and an error in the normalization was found [9], which overestimated the cross section by a factor of 100. The corrected cross sections are in agreement with the results reported in Ref. [7,8]. The goal of the present work was to repeat the measurement with an independent technique, using an active target and detector system that measures both the ^{26}Mg recoils from the $^{23}\text{Na}(\alpha, p)^{26}\text{Mg}$ reaction and the incoming ^{23}Na beam with the same detector, removing the need for a normalization common to all previous measurements.

Another important mechanism in the production of ^{26}Al is the $^{23}\text{Na}(\alpha, n)^{26}\text{Al}$ reaction. Refs. [10–12] reported on the study of the $^{23}\text{Na}(\alpha, n)^{26}\text{Al}$ reaction. The data of Refs. [10,11] agree with each other, but are a factor of 3 higher than the

* mavila@anl.gov

cross sections of Ref. [12]. The NACRE compilation [13] used these three data sets for the calculation of the $^{23}\text{Na}(\alpha, n)^{26}\text{Al}$ reaction rate. Since the work of Ref. [12] performed time-of-flight measurements, they were considered more reliable, and thus the reaction rate reported in Ref. [13] used these data and renormalized the cross sections of Refs. [10,11] downward by a factor of 3.

In addition to the $^{23}\text{Na}(\alpha, n)^{26}\text{Al}$ reaction, its time-inverse reaction $^{26}\text{Al}(n, \alpha)^{23}\text{Na}$ is one of the dominant destruction mechanisms of ^{26}Al . The sensitivity studies performed in Ref. [3] have reported a strong dependence of the ^{26}Al yield on the $^{26}\text{Al}(n, \alpha)^{23}\text{Na}$ reaction. The experimental efforts measuring this reaction have mainly focused on the time-inverse $^{23}\text{Na}(\alpha, n)^{26}\text{Al}$ reaction, because of difficulties associated with the fabrication of a radioactive ^{26}Al target. The work of Refs. [10–12] used their previously mentioned measurements of the $^{23}\text{Na}(\alpha, n)^{26}\text{Al}$ reaction and applied the principle of detailed balance to obtain the contribution of the $^{26}\text{Al}(n_0, \alpha)^{23}\text{Na}$ reaction. A disadvantage of studying the time-inverse reaction is that it only provides information of the ground state transition of ^{23}Na , and contributions from excited states have to be calculated using theoretical models. However, the study of this reaction can be used to apply constraints to the $^{26}\text{Al}(n, \alpha)^{23}\text{Na}$ reaction.

In the present work the $^{23}\text{Na}(\alpha, p)^{26}\text{Mg}$ and $^{23}\text{Na}(\alpha, n)^{26}\text{Al}$ reactions are measured simultaneously. Thus, problems related to different detection systems, efficiencies, and normalization of the cross sections are avoided. The following sections describe the experimental method and the results of the measurements of the $^{23}\text{Na}(\alpha, p)^{26}\text{Mg}$ and $^{23}\text{Na}(\alpha, n)^{26}\text{Al}$ reactions. A comparison with previous measurements and theoretical calculations is also provided.

II. EXPERIMENTAL SETUP

The experiment was carried out at the ATLAS accelerator at Argonne National Laboratory. The data were measured using a multisampling ionization chamber (MUSIC) detector with a close to 100% detection efficiency. This detector has previously been used for measurements of fusion reactions of astrophysical interest [14]. MUSIC is an active target system with 18 anode strips allowing the measurement of an excitation function covering a large energy range. A full description of the detector and a more detailed explanation of the operation principles can be found in Ref. [15]. The technique for the measurement of α -particle induced reactions has been benchmarked with the $^{17}\text{O}(\alpha, n)^{20}\text{Ne}$ reaction, for which cross sections can be found in the literature [16]. More details about the data analysis of (α, p) and (α, n) reactions (including the $^{23}\text{Na} + ^4\text{He}$ system discussed in the present work) as well as verification of the technique will be published in a separate paper [17].

The experiment was performed in inverse kinematics using ^{23}Na beams with energies of 51.5 and 57.4 MeV, and intensities up to 5000 particles/second. To reduce the beam intensity, a series of pepper-pot attenuators [18] and the ATLAS beam sweeper, which increased the pulse period of the beam from 82 ns to 41 μs , were used. The beam was delivered to the MUSIC detector which was filled with 403 and 395 Torr of ^4He

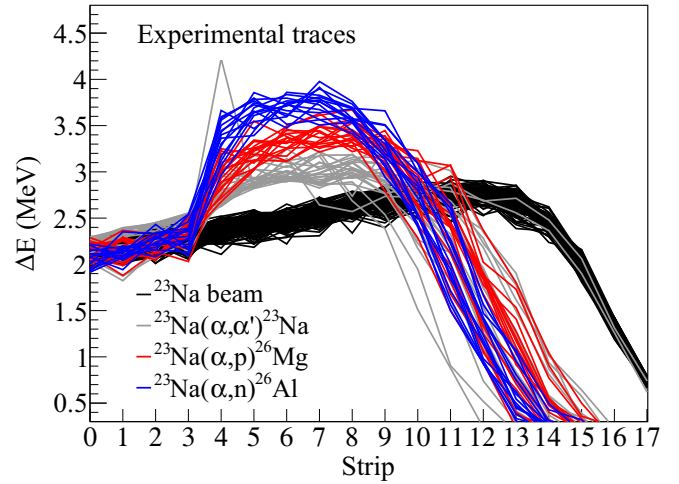


FIG. 1. Energy-loss signals measured in the 18 strips of the MUSIC detector for events of the $^{23}\text{Na}(\alpha, n)^{26}\text{Al}$ (blue), $^{23}\text{Na}(\alpha, p)^{26}\text{Mg}$ (red), and $^{23}\text{Na}(\alpha, \alpha')^{23}\text{Na}$ (gray) reactions occurring in strip 4. The black lines originate from the ^{23}Na beam.

gas for the lower and higher energy measurement, respectively. With these combinations of energies and pressures, an energy range in the center of mass of $E_{c.m.} = 2.2\text{--}5.8$ MeV was covered. In this energy range, both (α, p) ($Q = 1.820$ MeV) and (α, n) ($Q = -2.967$ MeV) channels are open, allowing us to measure the $^{23}\text{Na}(\alpha, p)^{26}\text{Mg}$ and $^{23}\text{Na}(\alpha, n)^{26}\text{Al}$ reactions simultaneously.

The separation of events from the two reactions is performed by analyzing the differences in the energy loss (ΔE) of the reaction products in each strip of the detector. For example, the ΔE for reactions occurring in strip 4 for a one-hour run from the higher beam energy measurement are shown in Fig. 1. In this figure, four groups of traces with different ΔE values, which originate from the ^{23}Na beam (black), the (α, p) reaction (red), the (α, n) reaction (blue), and from elastic and inelastic scattering reaction (gray), are visible. For a better visualization only the first 25 events of the (α, α') reaction are shown. The energy of the ^{23}Na ions passing through strip 0 was about 39 MeV, and for a pressure of 395 Torr the beam was almost stopped at strip 16, as can be seen in Fig. 1. The experimental traces seen in Fig. 1 are in agreement with simulated traces [17].

To improve the separation of the three reactions we have averaged the ΔE values over a certain number of strips following the strip where the reaction took place. This is done in order to avoid misinterpretation of the data due to fluctuations of the ΔE values measured in different strips of the detector. The average is called Av_n , with n indicating the number of strips used to calculate the average. The number of strips taken to perform the average is determined by the number of strips after the reaction takes place (rise of the trace) and before the reaction products stop in the chamber (fall of the trace). This method is explained in more detail in Ref. [17]. In Fig. 2, a two-dimensional plot of a five-strip average (Av_5) against a four-strip average (Av_4) for the whole 1.5 days long run is shown. The sharp cut seen in this figure at 2.3 MeV in the x axis (Av_5) is due to a pulse height condition

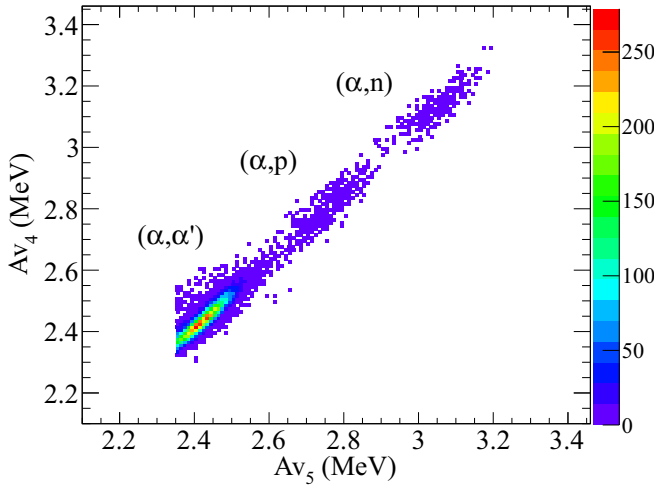


FIG. 2. Two-dimensional plot of ΔE values for events occurring in strip 4, averaged over five (Av_5) and four strips (Av_4) in order to improve the separation of events from the $^{23}\text{Na}(\alpha, \alpha')^{23}\text{Na}$, the $^{23}\text{Na}(\alpha, p)^{26}\text{Mg}$, and the $^{23}\text{Na}(\alpha, n)^{26}\text{Al}$ reactions.

applied to the data in order to discard the beamlike events. In this figure, the three groups originating from (α, α') , (α, p) , and (α, n) reactions are clearly distinguishable.

With this approach the cross sections of the $^{23}\text{Na}(\alpha, p)^{26}\text{Mg}$ and $^{23}\text{Na}(\alpha, n)^{26}\text{Al}$ reactions have been determined covering the energy range $E_{c.m.} \approx 2\text{--}6$ MeV in the center-of-mass frame. The normalization of the cross section is performed by using the number of beam particles (black traces in Fig. 1) which are simultaneously measured in the detector.

III. RESULTS

The excitation functions of angle- and excitation-energy-integrated cross sections of the $^{23}\text{Na}(\alpha, p)^{26}\text{Mg}$ and $^{23}\text{Na}(\alpha, n)^{26}\text{Al}$ reactions were measured in two runs lasting about 1.5 days each for the higher and lower energies. The results are presented in Fig. 3, where the (α, p) data are shown by red circles for the lower beam energy and by red triangles for the higher beam energy. Similarly, the (α, n) cross sections are shown by blue diamonds for the lower energy and blue squares for the higher beam energy, respectively. The uncertainties in the cross sections are statistical and the uncertainties in the center-of-mass energy are due to the energy range in each anode strip. The dashed lines are the cross sections predicted for the two reactions by the statistical-model from Ref. [19] using the TALYS code. The energy in the middle of each strip was calculated using the energy loss values of the code SRIM (version 2008) [20]. If the energy loss values are taken from the LISE++ prediction [21], there is an energy difference of about 10% on average. For the data points in Fig. 3, an effective energy was calculated instead of using the energy in the middle of each strip in order to take into account the energy dependence of the cross section. The energy width of a given strip averages the cross section over ~ 320 keV for the first strips and ~ 420 keV for the last strips in the center-of-mass system.

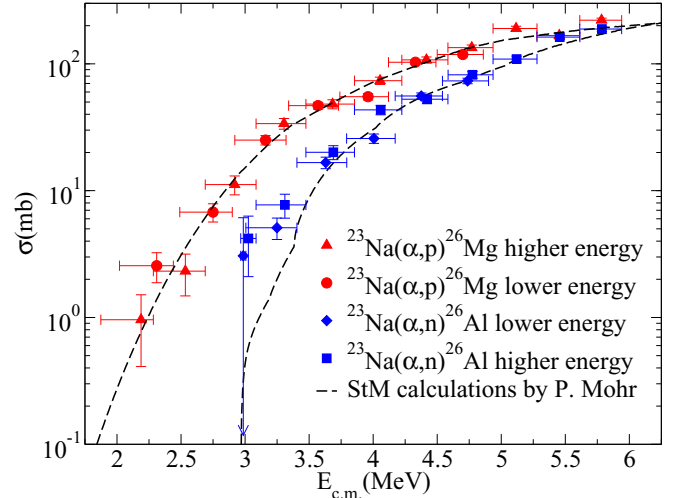


FIG. 3. Excitation functions of the $^{23}\text{Na}(\alpha, n)^{26}\text{Al}$ (blue) and the $^{23}\text{Na}(\alpha, p)^{26}\text{Mg}$ (red) reactions measured with the MUSIC detector for beam energies of 51.5 and 57.4 MeV, labeled as low energy and high energy, respectively.

A. The $^{23}\text{Na}(\alpha, p)^{26}\text{Mg}$ reaction

The $^{23}\text{Na}(\alpha, p)^{26}\text{Mg}$ reaction was previously studied in the center-of-mass range of about 1.7–3 MeV. Our experiment overlaps with previous measurements in the energy range of about 2–3 MeV. The cross section obtained in this work is found to be in good agreement with the experiments of Refs. [7–9] and with the statistical-model calculations of Ref. [19]. Moreover, our experiment was able to extend the measurements towards higher energies (up to 6 MeV) where no experimental data existed. In this energy region we again notice that the cross sections measured are in good agreement with the statistical-model calculations from Ref. [19]. A comparison of the $^{23}\text{Na}(\alpha, p)^{26}\text{Mg}$ cross sections from this experiment with previous measurements is presented in Fig. 4.

Our work confirms the cross sections and the reaction rates obtained in previous experiments and from statistical-model calculations.

B. The $^{23}\text{Na}(\alpha, n)^{26}\text{Al}$ reaction

In our experiment we have measured the $^{23}\text{Na}(\alpha, n)^{26}\text{Al}$ reaction together with the $^{23}\text{Na}(\alpha, p)^{26}\text{Mg}$ reaction. The $^{23}\text{Na}(\alpha, n)^{26}\text{Al}$ has been studied previously in several experiments [10–12]. Figure 5 gives a comparison of the total cross sections of the $^{23}\text{Na}(\alpha, n)^{26}\text{Al}$ reaction obtained in this work with previous measurements by Norman *et al.* [10], Skelton *et al.* [11], Doukellis and Rapaport [12], and statistical-model calculations performed by Mohr [19]. While the data of Norman *et al.* [10] and Skelton *et al.* [11] were taken from the EXFOR database [22], the data of Doukellis and Rapaport [12] are not available in the database and were therefore digitized using the program WEBPLOTDIGITIZER [23]. The cross sections of Refs. [10,11], taken in small energy steps, are shown by the small symbols. The averages of the data over the energy width of an individual strip of the MUSIC detector are represented by the larger symbols. A good agreement is observed between the

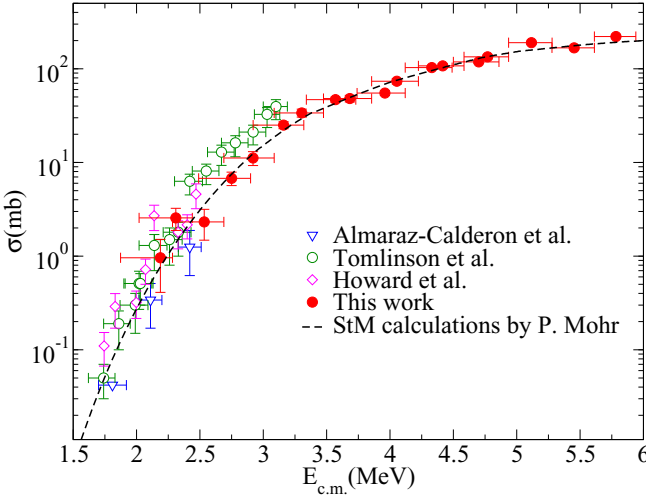


FIG. 4. Excitation functions of the $^{23}\text{Na}(\alpha, p)^{26}\text{Mg}$ reaction obtained in this work (red solid circles), in comparison with the results from Almaraz-Calderon *et al.* [9] (blue triangles), Tomlinson *et al.* [7] (green open circles), Howard *et al.* [8] (magenta diamonds), and the statistical-model calculations from Mohr [19].

cross sections of our study using the MUSIC detector and the experiments of Refs. [10,11], as well as with statistical-model predictions. However, they are about a factor of 3 higher than the results of Ref. [12]. Therefore, our work confirms the total cross section measured in Refs. [10,11] and disagrees with the results of Ref. [12].

Given the recommended rate [13] was calculated using the results of [12] and renormalized to the datasets of Refs. [10,11], we have performed a reevaluation of the $^{23}\text{Na}(\alpha, n)^{26}\text{Al}$

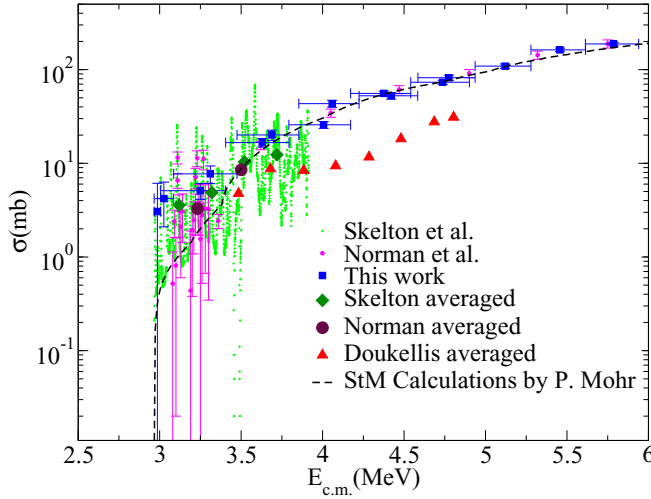


FIG. 5. Excitation functions of the $^{23}\text{Na}(\alpha, n)^{26}\text{Al}$ reaction obtained in this work (blue squares), by Norman *et al.* [10] (small magenta circles) with their energy-averaged values (large maroon circles), and by Skelton *et al.* [11] (small light green diamonds) with their energy-averaged values (large dark green diamonds). For Doukellis and Rapaport [12] only the energy-averaged values (large red triangles) are shown. The dashed line represents the statistical-model calculations by Mohr [19].

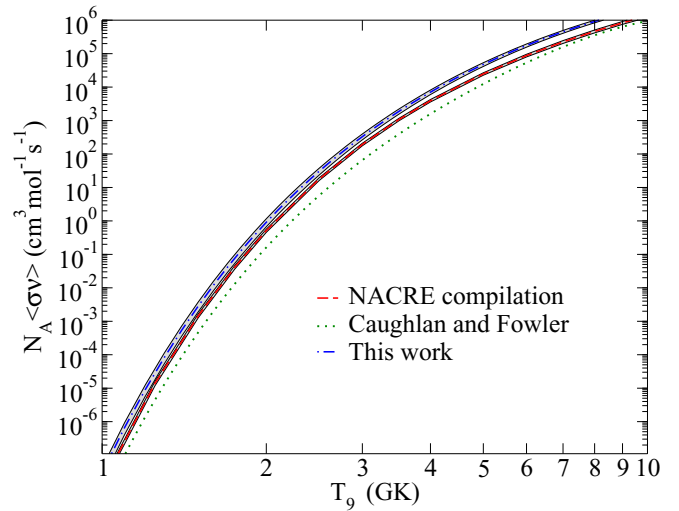


FIG. 6. The $^{23}\text{Na}(\alpha, n)^{26}\text{Al}$ reaction rate calculated in this work (dash-dotted line), in the NACRE compilation (dashed line) [13], and by Caughlan and Fowler [25] (dotted line). The grey area represents the error band.

reaction rate. To determine the reaction rate from the experimental cross sections of this work the computer code EXP2RATE [24] has been used. Figure 6 shows a comparison of the reaction rates from Caughlan and Fowler [25], the NACRE compilation [13], and the present work. As can be seen from Fig. 6 the reaction rate obtained in this work is higher than both the NACRE compilation and the one from Ref. [25]. With the parametrization from Ref. [26] the astrophysical reaction rate of the $^{23}\text{Na}(\alpha, n)^{26}\text{Al}$ reaction is given by

$$N_A \langle \sigma v \rangle = \exp[a_0 + a_1 T_9^{-1} + a_2 T_9^{-1/3} + a_3 T_9^{1/3} + a_4 T_9 + a_5 T_9^{5/3} + a_6 \ln(T_9)], \quad (1)$$

with T_9 being the temperature in GK; the reaction rate is in $\text{cm}^3 \text{mol}^{-1} \text{s}^{-1}$. To reproduce the reaction rate calculated in this work, we found that the constant values of $a_0 = 15.71$, $a_1 = -33.02$, $a_2 = a_3 = a_4 = a_5 = 0$, and $a_6 = 1.02$ give the best fit, with a χ^2 below 1. The implications of the larger $^{23}\text{Na}(\alpha, n)^{26}\text{Al}$ reaction rate calculated in this work, for the ^{26}Al abundance in massive stars, are difficult to estimate and are beyond the scope of this work. While a larger reaction rate suggests a larger production of ^{26}Al , it also implies more neutrons are available for other reactions that destroy ^{26}Al . Therefore, in order to determine the effect of a larger reaction rate of the $^{23}\text{Na}(\alpha, n)^{26}\text{Al}$ reaction for the ^{26}Al production, new theoretical stellar model calculations are required.

IV. SUMMARY

We have performed a simultaneous measurement of excitation functions of the $^{23}\text{Na}(\alpha, p)^{26}\text{Mg}$ and $^{23}\text{Na}(\alpha, n)^{26}\text{Al}$ reactions, which are important for the understanding of ^{26}Al production in massive stars. The experiment was carried out by making use of a multisampling ionization chamber and the advantages of inverse kinematics, which gives $\sim 100\%$ detection efficiency of the reaction products. The cross sections

measured for the $^{23}\text{Na}(\alpha, p)^{26}\text{Mg}$ reaction were found to be in good agreement with previous measurements as well as with statistical-model calculations. Furthermore, the cross section of the $^{23}\text{Na}(\alpha, p)^{26}\text{Mg}$ reaction was extended to higher energies. Discrepancies of the cross sections for the $^{23}\text{Na}(\alpha, p)^{26}\text{Mg}$ reactions in previous measurements have now been settled. Our measurement of the $^{23}\text{Na}(\alpha, n)^{26}\text{Al}$ reaction is in agreement with the measurements of Refs. [10,11] and about a factor of 3 higher than the cross section measured in Ref. [12]. A revised reaction rate has been calculated which is higher than what was previously recommended.

In addition, we have presented a technique to measure simultaneously excitation functions of angle- and excitation-energy-integrated cross sections of (α, p) and (α, n) reactions. Because the beam particles and the reaction products are measured in the same detector, problems with normalization of

the cross section are avoided. This is an efficient way to study astrophysically important reactions because a large range of the excitation function for two different reactions is covered with a single beam energy.

ACKNOWLEDGMENTS

The authors are grateful to Dr. P. Mohr for helpful discussions. This material is based upon work supported by the U.S. Department of Energy, Office of Science, Office of Nuclear Physics, under Contract No. DE-AC02-06CH11357. The authors J.L. and D.S.G. acknowledge the support by the U.S. Department of Energy, Office of Science, Office of Nuclear Science, under Grant No. DE-FG02-96ER40978. This research used resources of ANL's ATLAS facility, which is DOE Office of Science User Facility.

-
- [1] R. Diehl, C. Dupraz, K. Bennett, H. Bloemen, W. Hermsen, J. Knöldlseder, G. Lichten, D. Morris, J. Ryan, V. Schönfelder, H. Steinle, A. Strong, B. Swanenburg, M. Varendorff, and C. Winkler, *Astron. Astrophys.* **298**, 445 (1995).
 - [2] R. Diehl, H. Halloin, K. Kretschmer, G. G. Lichten, V. Schönfelder, A. W. Strong, A. von Kienlin, W. Wang, P. Jean, J. Knöldlseder, J.-P. Roques, G. Weidenspointner, S. Schanne, D. H. Hartmann, C. Winkler, and C. Wunderer, *Nature (London)* **439**, 45 (2006).
 - [3] C. Iliadis, A. Champagne, A. Chieffi, and M. Limongi, *Astrophys. J. Suppl.* **193**, 16 (2011).
 - [4] J. Kuperus, *Physica (Amsterdam)* **30**, 2253 (1964).
 - [5] D. P. Whitmire and C. N. Davids, *Phys. Rev. C* **9**, 996 (1974).
 - [6] S. Almaraz-Calderon, P. F. Bertone, M. Alcorta, M. Albers, C. M. Deibel, C. R. Hoffman, C. L. Jiang, S. T. Marley, K. E. Rehm, and C. Ugalde, *Phys. Rev. Lett.* **112**, 152701 (2014).
 - [7] J. R. Tomlinson, J. Fallis, A. M. Laird, S. P. Fox, C. Akers, M. Alcorta, M. A. Bentley, G. Christian, B. Davids, T. Davinson, B. R. Fulton, N. Galinski, A. Rojas, C. Ruiz, N. de Séreville, M. Shen, and A. C. Shotter, *Phys. Rev. Lett.* **115**, 052702 (2015).
 - [8] A. M. Howard, M. Munch, H. O. U. Fynbo, O. S. Kirsebom, K. L. Laursen, C. A. Diget, and N. J. Hubbard, *Phys. Rev. Lett.* **115**, 052701 (2015).
 - [9] S. Almaraz-Calderon, P. F. Bertone, M. Alcorta, M. Albers, C. M. Deibel, C. R. Hoffman, C. L. Jiang, S. T. Marley, K. E. Rehm, and C. Ugalde, *Phys. Rev. Lett.* **115**, 179901(E) (2015).
 - [10] E. B. Norman, E. C. Timothy, K. T. Lesko, and S. Peter, *Nucl. Phys. A* **390**, 561 (1982).
 - [11] R. T. Skelton, R. W. Kavanagh, and D. G. Sargood, *Phys. Rev. C* **35**, 45 (1987).
 - [12] G. Doukellis and J. Rapaport, *Nucl. Phys. A* **467**, 511 (1987).
 - [13] C. Angulo, M. Arnould, M. Rayet, P. Descouvemont, D. Baye, C. Leclercq-Willain, A. Coc, S. Barhoumi, P. Aguer, C. Rolfs, R. Kunz, J. W. Hammer, A. Mayer, T. Paradellis, S. Kossionides, C. Chronidou, K. Spyrou, S. Degl'Innocenti, G. Florentini, B. Ricci, S. Zavatarelli, C. Providencia, H. Wolters, J. Soares, C. Grama, J. Rahighi, A. Shotter, and M. Lamehi Rachti, *Nucl. Phys. A* **656**, 3 (1999).
 - [14] P. F. F. Carnelli, S. Almaraz-Calderon, K. E. Rehm, M. Albers, M. Alcorta, P. F. Bertone, B. Digiovine, H. Esbensen, J. O. Fernández Niello, D. Henderson, C. L. Jiang, J. Lai, S. T. Marley, O. Nusair, T. Palchan-Hazan, R. C. Pardo, M. Paul, and C. Ugalde, *Phys. Rev. Lett.* **112**, 192701 (2014).
 - [15] P. F. F. Carnelli, S. Almaraz-Calderon, K. E. Rehm, M. Albers, M. Alcorta, P. F. Bertone, B. Digiovine, H. Esbensen, J. Fernández Niello, D. Henderson, C. L. Jiang, J. Lai, S. T. Marley, O. Nusair, T. Palchan-Hazan, R. C. Pardo, M. Paul, and C. Ugalde, *Nucl. Instrum. Methods Phys. Res. Sect. A* **799**, 197 (2015).
 - [16] J. K. Bair and F. X. Haas, *Phys. Rev. C* **7**, 1356 (1973).
 - [17] M. L. Avila, K. E. Rehm, S. Almaraz-Calderon, A. D. Ayangeakaa, C. Dickerson, C. R. Hoffman, C. L. Jiang, B. P. Kay, J. Lai, O. Nusair, R. C. Pardo, D. Santiago-Gonzalez, R. Talwar, and C. Ugalde, [arXiv:1608.03290](https://arxiv.org/abs/1608.03290).
 - [18] P. W. Kubik, D. Elmore, T. K. Hemmick, H. E. Gove, U. Fehn, R. T. Teng, S. Jiang, and S. Tullai, *Nucl. Instrum. Methods Phys. Res. Sect. B* **29**, 138 (1987).
 - [19] P. Mohr, *Europhys. J. A* **51**, 1 (2015), and private communication.
 - [20] J. F. Ziegler, M. D. Ziegler, and J. P. Biersack, *Nucl. Instrum. Methods Phys. Res. Sect. B* **268**, 1818 (2010).
 - [21] O. B. Tarsov and D. Bazin, *Nucl. Instrum. Methods Phys. Res. Sect. B* **266**, 4657 (2008).
 - [22] N. Otuka, E. Dupont, V. Semkova, B. Pritychenko, A. I. Blokhin, M. Aikawa, S. Babykina, M. Bossant, G. Chen, S. Dunaeva, R. A. Forrest, T. Fukahori, N. Furutachi, S. Ganesan, Z. Ge, O. O. Gritzay, M. Herman, S. Hlavač, K. Katō, B. Lalremruata, Y. O. Lee, A. Makinaga, K. Matsumoto, M. Mikhaylyukova, G. Pikulina, V. G. Pronyaev, A. Saxena, O. Schwerer, S. P. Simakov, N. Soppera, R. Suzuki, S. Takács, X. Tao, S. Taova, F. Tárkányi, V. V. Varlamov, J. Wang, S. C. Yang, V. Zerkin, and Y. Zhuang, *Nucl. Data Sheets* **120**, 272 (2014).
 - [23] A. Rohatgi, WEBPLOTDIGITIZER Version 3.10, <http://arohatgi.info/WebPlotDigitizer>.
 - [24] T. Rauscher, code EXP2RATE, <http://download.nucastro.org/codes/exp2rate.f90>.
 - [25] G. R. Caughlan and W. A. Fowler, *At. Data Nucl. Data Tables* **40**, 283 (1988).
 - [26] T. Rauscher and F.-K. Thielemann, *At. Data Nucl. Data Tables* **75**, 1 (2000).